frontiers | Frontiers in Earth Science

ORIGINAL RESEARCH
published: 22 June 2022
doi: 10.3389/feart.2022.938323

Earth's Orbital Control on Organic Matter Enrichment in the Black Shales of the Wufeng–Longmaxi Formation in the Upper Yangtze Region, South China

Shaoze Zhao[1,2], *Yong Li*[1]*, *Yingjiao Xu*[3], *Leli Cheng*[4], *Zhou Nie*[5] *and Liang Zhao*[1]

[1]College of Earth Sciences, Chengdu University of Technology, Chengdu, China, [2]Postdoctoral Research Station of Geology, Chengdu University of Technology, Chengdu, China, [3]College of Earth Sciences, Hebei GEO University, Shijiazhuang, China, [4]Institute of Logging Technology and Engineering, Yangtze University, Jingzhou, China, [5]PetroChina Southwest Oil and Gas Field Company, Chengdu, China

OPEN ACCESS

Edited by:
Yu Song,
China University of Geosciences (Wuhan), China

Reviewed by:
Juye Shi,
China University of Geosciences (Beijing), China
Dongdong Wang,
Shandong University of Science and Technology, China
Ping Gao,
China University of Geosciences (Beijing), China

***Correspondence:**
Yong Li
liy@cdut.edu.cn

Specialty section:
This article was submitted to Geochemistry, a section of the journal Frontiers in Earth Science

Received: 07 May 2022
Accepted: 30 May 2022
Published: 22 June 2022

Citation:
Zhao S, Li Y, Xu Y, Cheng L, Nie Z and Zhao L (2022) Earth's Orbital Control on Organic Matter Enrichment in the Black Shales of the Wufeng–Longmaxi Formation in the Upper Yangtze Region, South China. Front. Earth Sci. 10:938323. doi: 10.3389/feart.2022.938323

China's most successful horizon for shale-gas exploration and development is the Upper Ordovician Wufeng Formation through the Lower Silurian Longmaxi Formation in its Upper Yangtze Region. In this study, the Wufeng–Longmaxi Formation black shales in the Upper Yangtze Region are analysed to determine their microstructural characteristics, total organic carbon (TOC) content, and well log characteristics and to identify information on the parameters of Earth's orbit from its gamma-ray (GR) data series. Then, paleoenvironmental modes are established over a long time scale. On this basis, the Earth's orbital control on organic matter enrichment in the black shales is examined. The black shales of the Wufeng Formation and the lower Longmaxi Formation are rich in biogenic siliceous fossils and framboidal pyrite. Their TOC content, GR value, and uranium (U) content increase gradually from the bottom of the Wufeng Formation to the Guanyinqiao Member at its top, peak at the Guanyinqiao Member, and then decrease gradually up to the Longmaxi Formation. Approximately six and seven long eccentricity cycles can be identified from the GR curves of the Wufeng Formation and the lower Longmaxi Formation, respectively. During the long eccentricity minima, corresponding to Earth's cold period, the black shales have a relatively high level of enrichment of organic matter. This study can provide an important reference for investigating the mechanism by which Earth's orbits control the climate and sedimentary environment, as well as the mechanism of organic matter enrichment.

Keywords: black shales, Wufeng-Longmaxi formation, upper yangtze region, Earth's orbit parameters, orbital control on organic matter enrichment

HIGHLIGHTS

- The black shales in the Upper Ordovician Wufeng Formation through the Lower Silurian Longmaxi Formation are rich in biogenic siliceous fossils and framboidal pyrite.
- The total organic carbon (TOC) content, gamma-ray (GR) value, and uranium (U) content overall increase gradually from the bottom of the Wufeng Formation to the Guanyinqiao

Member at its top, peak at the Guanyinqiao Member, and then decrease gradually up to the Longmaxi Formation.
- Approximately six and seven long eccentricity cycles can be identified from the GR curves of the Wufeng Formation and the lower Longmaxi Formation, respectively.
- The black shales have a relatively high level of enrichment of organic matter at long eccentricity minima and a relatively low level at long eccentricity maxima.

1 INTRODUCTION

Periodic changes in the parameters (i.e., eccentricity, obliquity, and precession) of Earth's orbit lead to periodic fluctuations in the amount of solar radiation and thus the surface climatic system on Earth. These periodic climatic changes are recorded in sediments sensitive to climate change, resulting in cyclic features in sedimentary formations, known as Milankovitch cycles (Schwarzacher, 1989; Schwarzacher, 1993; Strasser et al., 2006). Researchers have identified Milankovitch cycles (or Earth's orbital parameters) in sedimentary formations using metrics reflective of palaeoclimatic changes, such as carbon and oxygen isotopes, gamma-ray (GR) values, magnetic susceptibility, organic carbon, and element ratios in conjunction with methods such as wavelet and spectral analysis (Weedon et al., 2004; Sageman et al., 2006; Huang et al., 2010; Cheng et al., 2017; Jin S. et al., 2020; Ravier et al., 2020; Shi et al., 2020; Shi et al., 2021; Kochhanna et al., 2021; Zhang et al., 2021). Analysis of Earth's orbital parameters in sedimentary formations has produced a series of progress, e.g., the improvement of the International Geological Time Scale (Lourens et al., 2004), the estimation of the duration and rate of deposition of formations (Huang et al., 2010; Cheng et al., 2017), the estimation of the duration of major geological events and the determination of their trigger mechanisms (Sageman et al., 2006; Zhong et al., 2020), and the recognition of the effects of orbits on sedimentary environments (Weedon et al., 2004; Yao et al., 2015; Jin S. et al., 2020; Ravier et al., 2020; Shi et al., 2020; Shi et al., 2021; Kochhanna et al., 2021; Zhang et al., 2021).

Rachold and Brumsack (2001) summarized some effects of Earth's orbits on climatic processes and sedimentary environments (including sea-level changes, weathering processes, organic productivity, and reduction–oxidation conditions). However, the mechanisms by which orbits control sedimentary environments have yet to be understood. For example, research on the mechanism by which orbits affected the sedimentary environment and organic matter enrichment in Palaeozoic shales stagnates in only two hypothetical models. 1) The eccentricity cycle controls primary productivity. This model states that during maximum eccentricity, intense weathering causes oceanward transport of terrestrial detritus and nutrients in large quantities and thereby aids in increasing oceanic primary productivity. That is, a high level of enrichment of organic matter occurred in shales during maximum eccentricity. 2) The eccentricity cycle controls organic matter preservation conditions. This model states that a change in seasons occurs less frequently during minimum eccentricity, thereby providing a stable sedimentary environment with relatively good preservation conditions for organic matter that allow for a high level of enrichment of organic matter in shales (Gambacorta et al., 2018; Jin S. et al., 2020).

Extraction of shale gas from the black shales of the Upper Ordovician Wufeng Formation and the Lower Silurian Longmaxi Formation in southern China's Yangtze Region has been a great success (Zou et al., 2018). Through relatively extensive investigations of the paleoenvironment during the deposition of the Wufeng–Longmaxi Formation black shales, previous researchers have noted that the Yangtze Sea had relatively high primary productivity and an anoxic bottom-water environment during this period (Li et al., 2017; Zhao et al., 2019; Jin C. et al., 2020; Yang S. et al., 2021; Zan et al., 2021). In addition, they have discussed the controlling factors of organic matter enrichment in the black shales of the Wufeng–Longmaxi Formation from multiple perspectives, including upwelling currents, volcanic ash, sea-level changes, and occlusive settings (Li et al., 2017; Zhao et al., 2019; Jin C. et al., 2020; Yang S. et al., 2021; Zan et al., 2021). Million-year-scale palaeo-ocean and palaeoclimate research findings show that while the shales in the Wufeng–Longmaxi Formation in the Yangtze Region are several hundred metres in thickness, organic matter-rich black shales are concentrated mainly within the bottom several tens of metres (Zou et al., 2018). Jin S. et al. (2020) and Zhang et al. (2021) identified the cycles of Earth's orbital parameters (e.g., eccentricity, obliquity, and precession) from the black shales of the Wufeng–Longmaxi Formation in the Upper Yangtze Region. The investigation of the Earth's orbital control on organic matter-rich enrichment in the black shales of the Wufeng–Longmaxi Formation is still in the exploratory stage.

To address the above problem, this study analyses black shales of the Wufeng–Longmaxi Formation in well N211 and the Shuanghe profile to determine their microscopic characteristics, total organic carbon (TOC) content, and well log characteristics. Information for the parameters of Earth's orbit contained in the black shales of the Wufeng–Longmaxi Formation is identified using the GR curves of well N211. Then, paleoenvironmental modes are established, and the controlling effects of a long eccentricity cycle on organic matter enrichment in the black shales are examined. This study can become an important reference for investigating the mechanisms by which Earth's orbits control climate and sedimentary environments and the mechanism of organic matter enrichment in black shales.

2 GEOLOGICAL SETTING

The Yangtze Block collided and merged with the Cathaysian Block during the Middle Ordovician to form the South China Block (Wang, 1985; Chen et al., 2004; Su et al., 2009). During the Late Ordovician through the early Silurian, the South China Block was situated in the equatorial tropical or subtropical region on the western margin of the Gondwana continent (**Figures 1A,B**) (Metcalfe, 1994; Li et al., 2005; Huang et al., 2018). In this period, the Central Sichuan Submarine Uplift and the Central Guizhou Uplift were formed on the western margin

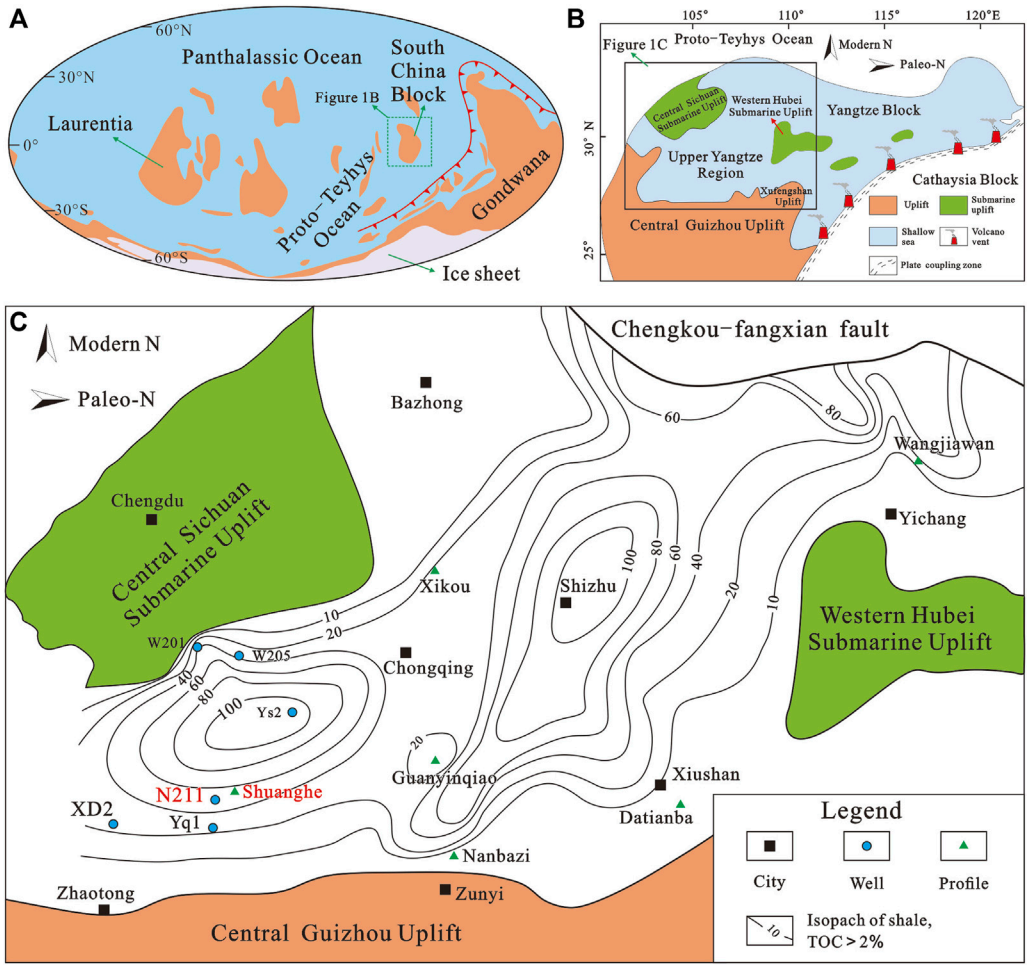

FIGURE 1 | Geological setting of the Upper Yangtze Region during the Late Ordovician through the Early Silurian. **(A)** Palaeogeographic location of the South China Block during the Late Ordovician through the Early Silurian. The South China Block was situated in the equatorial tropical or subtropical region on the western margin of the Gondwana continent at approximately 90° counterclockwise from its present-day location, according to Cocks and Torsvik (2002) and Huang et al. (2020). **(B)** Paleogeographic map of the Yangtze Block during the Late Ordovician through the Early Silurian. The present-day northern margin of the Yangtze Region was its western margin during the Late Ordovician through the Early Silurian. The Upper Yangtze Region is surrounded by the Central Sichuan Submarine Uplift, Central Guizhou Uplift, and Western Hubei Submarine Uplift, according to Zhou et al. (2015); Wang et al. (2017); Liu et al. (2017), and Tang et al. (2020). **(C)** Distribution of the organic matter-rich shales in the Wufeng–Longmaxi Formation in the Upper Yangtze Region. Those with a TOC > 2% have a thickness up to approximately 100 m, and the thickest organic-rich shales are near Shizhu and well Ys2, according to Wang et al. (2017).

and in the southern part of the Upper Yangtze Region, respectively, while the Xuefengshan Uplift and Western Hubei Submarine Uplift developed in the eastern part (**Figure 1B**). These factors led to the formation of an expansive, low-energy, and undercompensated sedimentary environment (Chen et al., 2004; Yan et al., 2009; Chen et al., 2013), where organic matter-rich black shales were deposited over a large area. Of these black shales, those with a TOC > 2% have a thickness of up to approximately 100 m (**Figure 1C**) (Wang et al., 2017).

With a lithological composition consisting primarily of siliceous shales (**Figure 2A**), the Wufeng Formation and the lower Longmaxi Formation in the Upper Yangtze Region are rich in graptolite fossils (**Figure 2B**) and are intercalated with thin pyrite layers (**Figure 2C**) and thin potash bentonite layers (**Figure 2D**). The Guanyinqiao Member at the top of the Wufeng Formation consists of three facies—siliceous shale facies, calcareous-siliceous shale facies, and limestone facies—in the Upper Yangtze Region (Wang et al., 2016). The siliceous and calcareous-siliceous shales contain an abundance of Hirnantian faunal fossils (**Figure 2E**), suggesting the presence of a cold, regressive, relatively shallow-water, and oxygen-rich sedimentary environment (Rong et al., 2010).

Chen et al. (2015) divided the Wufeng–Longmaxi Formation into 13 graptolite biozones, each with a corresponding isotopic age (**Figure 3A**). The organic matter-rich black shales are located in the Wufeng Formation and the lower Longmaxi Formation, primarily corresponding to the WF1–LM5 graptolite zones (Zou et al., 2018). Therefore, only the black shales in the

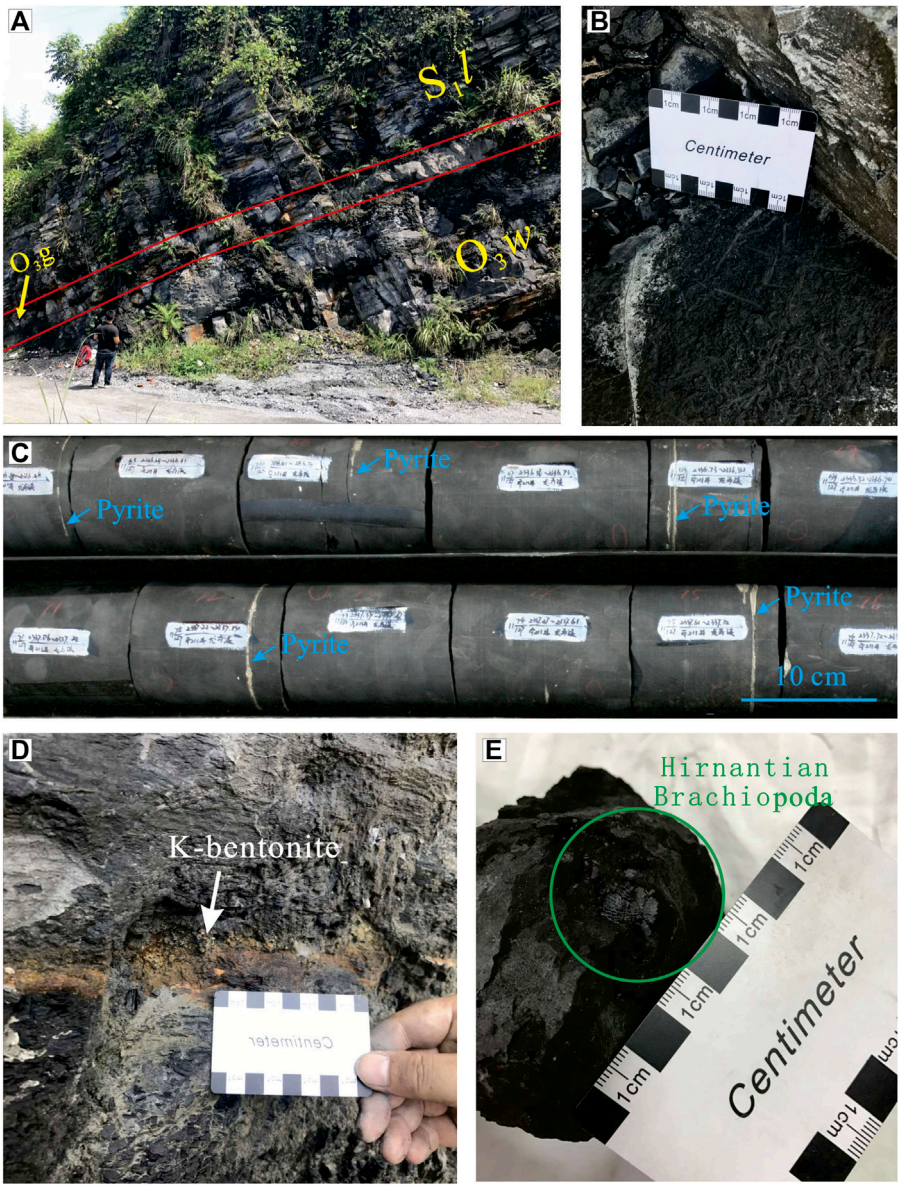

FIGURE 2 | Stratigraphic characteristics of the Wufeng–Longmaxi Formation, Upper Yangtze Region. **(A)** Continuous black siliceous shale deposits in the Wufeng Formation (O_3w) and Longmaxi Formation (S_1l); the Guanyinqiao Member (O_3g) at the top of the Wufeng Formation is approximately 1 m thick. **(B)** Graptolite-rich siliceous shales in the Wufeng Formation; graptolites are between 0.5 and 5 cm in length. **(C)** The black siliceous shale of the Longmaxi Formation contains multiple layers of pyrite with a thickness of a single layer less than 3 mm. **(D)** Potash bentonite intercalation with a thickness of less than 1 cm in the Wufeng Formation. **(E)** Hirnantian fossil in the siliceous shales of the Guanyinqiao Member; the fossil is approximately 2 cm in diameter. **(A, B, D, E)** Images of the Shuanghe profile; **(C)**, images of the well N211 cores.

Wufeng–Longmaxi Formation deposited during the deposition of the WF1–LM5 graptolite zones (i.e., during the Late Katian through the Rhuddanian) are discussed in this paper. The deposition time of the Wufeng Formation (Upper Katian–Lower Hirnantian) was between 3.19 and 3.79 Myr; the lower Longmaxi Formation (Upper Hirnantian–Rhuddanian), between 3.06 and 3.66 Myr (**Figure 3A**). These deposition times are only estimates because the isotopic ages of these formations generally have an error of 0.7–1.5 Myr (Gradstein et al., 2012). The Wufeng–Longmaxi Formation (Upper Katian–Rhuddanian) in well N211 in the Upper Yangtze Region is a continuous sedimentary formation composed of siliceous shales (**Figure 3B**). With a thickness of 9.7 m (2347.3–2357 m), the Wufeng Formation is in parallel unconformable contact with the underlying nodular limestones in the Baota Formation, and WF2–4 graptolite zones are fully developed in the Wufeng Formation (Luo et al., 2017). With a thickness of 1 m (2347.3–2348.3 m), the

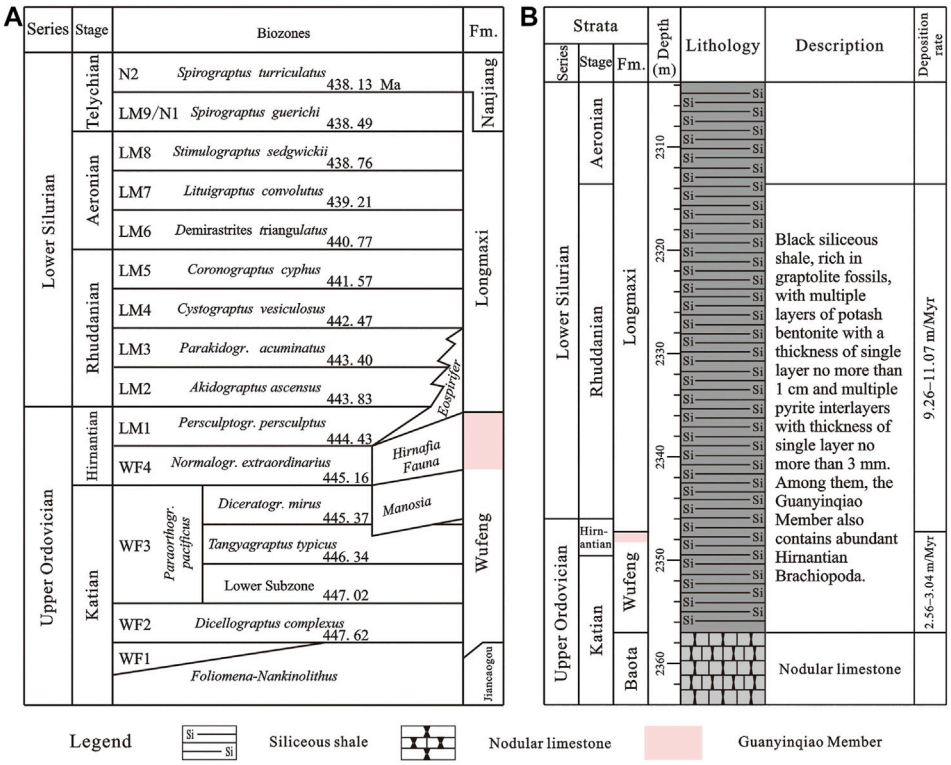

FIGURE 3 | (A) Graptolite biozones in the Wufeng–Longmaxi Formation in the Yangtze Region, according to Chen et al. (2015). **(B)** Stratigraphic column for well N211.

Guanyinqiao Member at the top of the Wufeng Formation contains many Hirnantian faunal fossils. The lower Longmaxi Formation (Upper Hirnantian–Rhuddanian) has a thickness of 33.86 m (2313.44–2347.3 m). The deposition rates are estimated based on the deposition times and thicknesses. The sedimentation rates of the Wufeng Formation and the lower Longmaxi Formation (Upper Hirnantian–Rhuddanian) in well N211 are 2.56–3.04 and 9.26–11.07 m/Myr, respectively (**Figure 3B**). All the black shales of the lower Longmaxi Formation in subsequent analyses refer to the Upper Hirnantian–Rhuddanian black shales.

3 SAMPLES, DATA, AND METHODS

3.1 Samples and Data

Five samples of the black shales of the Wufeng Formation and the lower Longmaxi Formation were collected from the Shuanghe profile and then analysed to determine their microstructural characteristics. Forty black shale samples were retrieved from the Wufeng Formation and the lower Longmaxi Formation in well N211 (9 from the Wufeng Formation (including 1 from the Guanyinqiao Member) and 31 from the lower Longmaxi Formation) for TOC analysis. Well log data [GR values and uranium (U) content, data point interval: 0.1524 m] were obtained by Schlumberger Limited from well N211. The GR values and U content were measured using natural gamma-ray spectral logging.

3.2 Microscopic Characteristics of the Shales and the Total Organic Carbon Analytical Method

The microscopic characteristics of the black shales were analysed using a Leica DM4500P polarized-light microscope and a Quanta 250 FEG scanning electron microscope at the State Key Laboratory of Oil and Gas Reservoir Geology and Exploitation, Chengdu University of Technology.

The black shale samples were ultrasonically washed multiple times in deionized water and then dried. Then, they were ground in an agate mortar and passed through an 80-mesh screen for TOC analysis, which was performed using a CS230 C–S analyser at the Analytical Experimental Centre of the Research Institute of Petroleum Exploration and Development, PetroChina Southwest Oil and Gas Field Company.

3.3 Spectral Analytical Method

The black shales in the Wufeng Formation and the lower Longmaxi Formation were deposited at fairly different rates. Therefore, the GR values retrieved from the Wufeng Formation and the lower Longmaxi Formation were separately subjected to spectral analysis using the Acycle 2.3.1 software

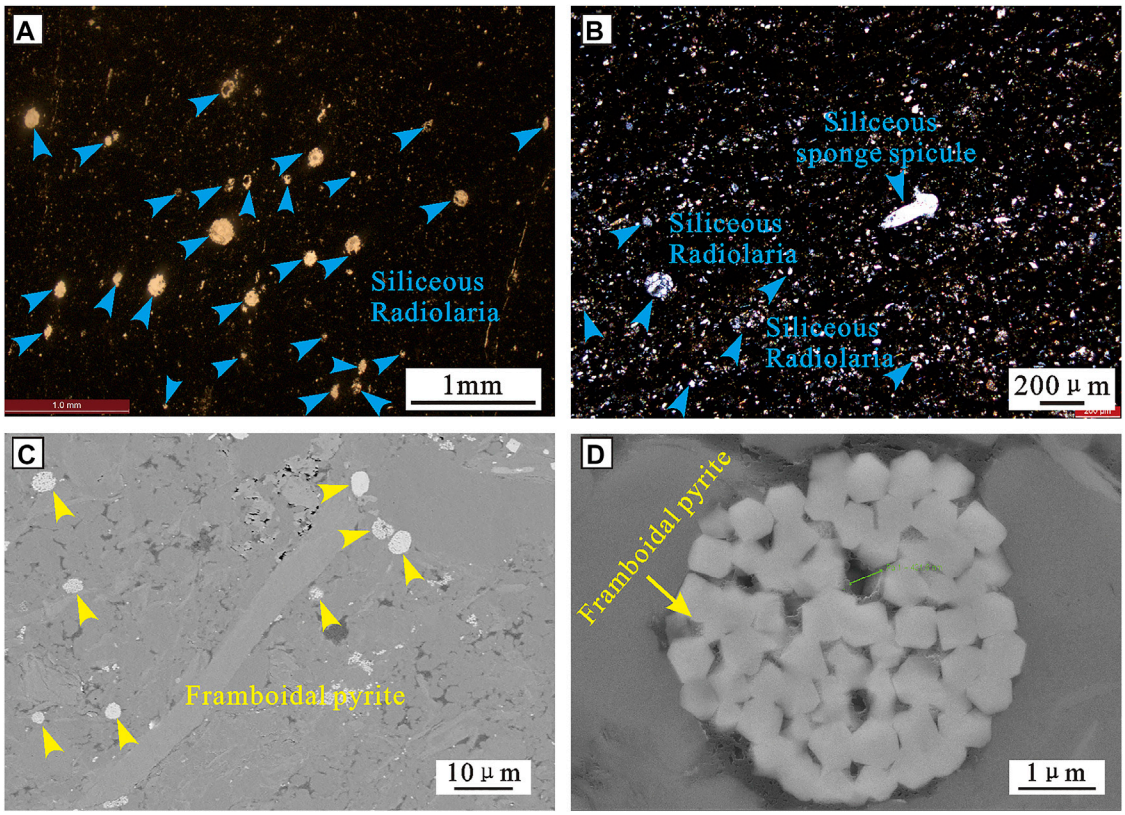

FIGURE 4 | Microscopic images of the black shales of the Wufeng Formation and the lower Longmaxi Formation in the Upper Yangtze Region. **(A)** Extensive presence of siliceous Radiolaria in the black shales, with diameters generally between 50 and 200 μm. **(B)** Siliceous sponge spicule and Radiolaria in the black shales, siliceous sponge spicule with a diameter of approximately 50 μm and length of approximately 300 μm, and siliceous Radiolaria with diameters of approximately 20–150 μm. **(C,D)** Framboidal pyrite in the black shales, with diameters generally between 2 and 5 μm **(A,B)** are polarized light microscopy images. **(C)** and **(D)** are scanning electron microscopy images.

package based on the MATLAB platform (Li et al., 2019). The main analytical methods involved in this study include multitaper-method spectral analysis and fast-Fourier transform sliding-window spectral analysis.

4 RESULTS

4.1 Microscopic Characteristics of the Shales

The black shales of the Wufeng Formation and the lower Longmaxi Formation are rich in biogenic siliceous fossils, including siliceous Radiolaria with diameters of generally less than 200 μm (**Figure 4A**) and sponge spicules with diameters of approximately 50 μm and lengths of approximately 300 μm (**Figure 4B**). Ma et al. (2018) suggested that sources of the siliceous matter in the Wufeng and lower Longmaxi Formation black shales include siliceous organisms (67–90%) and a small amount of terrestrial detritus. This finding, combined with the microscopic analysis conducted in this study, clearly shows that the siliceous components of the Wufeng and lower Longmaxi Formation black shales are primarily biogenic. Extensive framboidal pyrite with a particle diameter of less than 5 μm has developed in the Wufeng and lower Longmaxi Formation black shales (**Figures 4C,D**), suggesting that the bottom seawater or the porewater in the sediments had an anoxic environment during the deposition of these black shales (Bond and Wignall, 2010).

4.2 Total Organic Carbon Content

The black shales of the Wufeng and lower Longmaxi Formations have a high TOC content (**Figure 5**). The TOC content in the black shales of the Wufeng Formation ranges from 1.01% to 8.35% and increases gradually from the bottom up. Specifically, this TOC content is 1.01–5.75% (average: 3.66%) at the bottom-middle and 8.35% (the highest TOC content in the Wufeng and lower Longmaxi Formation black shales) in the Guanyinqiao Member at the top. In addition, the Guanyinqiao Member is rich in benthic fossils (i.e., Hirnantian fauna fossils), suggesting the presence of oxygen-rich bottom seawater during the deposition of the Guanyinqiao Member but the presence of anoxic porewater in the sediments in the Guanyinqiao Member. The TOC content in the lower Longmaxi Formation black shales ranges from 1.28% to 6.04% (average: 3.15%) and decreases gradually from the bottom up (**Figure 5**). The TOC content increases gradually from the bottom of the Wufeng Formation to its Guanyinqiao

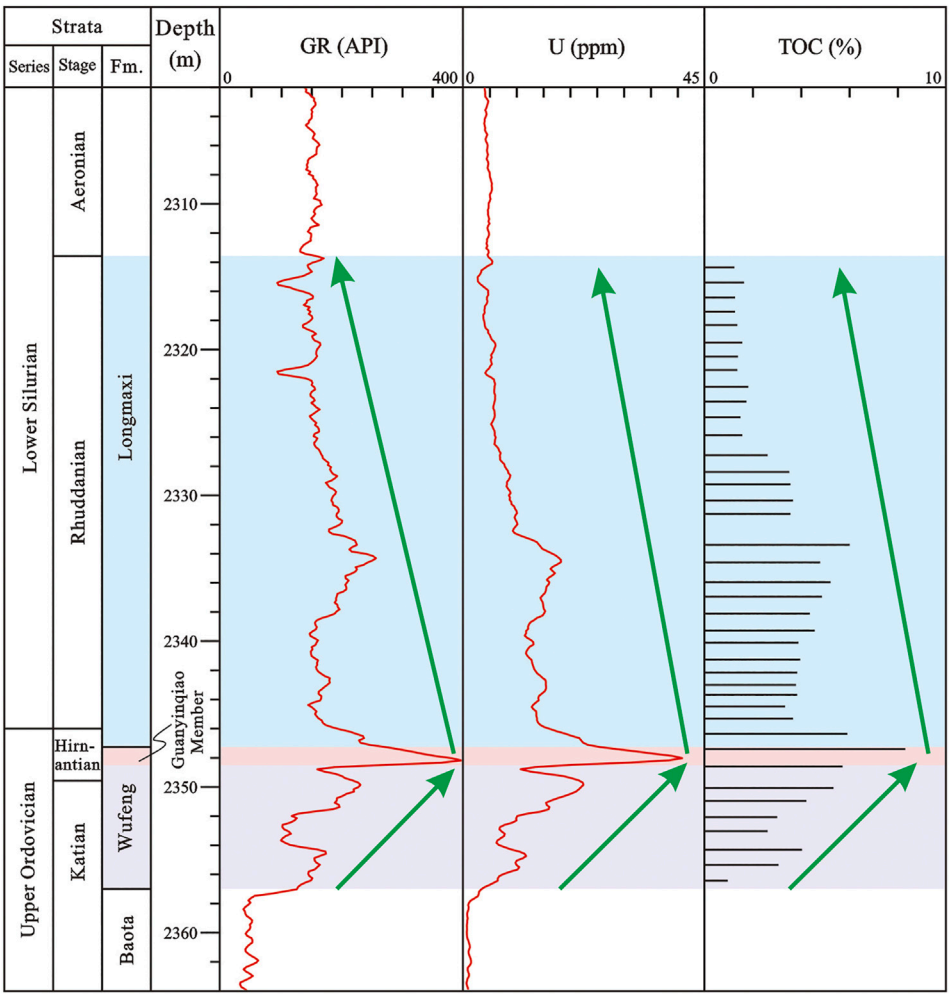

FIGURE 5 | TOC and well log characteristics of the Wufeng Formation and the lower Longmaxi Formation in well N211 in the Upper Yangtze Region.

Member, peaks in the Guanyinqiao Member, and then decreases gradually going further up to the Longmaxi Formation (**Figure 5**).

4.3 Well Log Characteristics

For the lower Wufeng Formation, the GR values range from 98.88 to 272.76 (average: 160.26) American Petroleum Institute (API) units, and the mass fractions of U are 3.96–22.40 ppm (average: 12.07 ppm). In the Guanyinqiao Member at the top of the Wufeng Formation, the GR value ranges from 294.59 to 397.58 (average: 348.79) API units, and the mass fractions of U are 28.78–40.81 ppm (average: 35.10 ppm). For the lower Longmaxi Formation, the GR value ranges from 92.77 to 273.29 (average: 170.06) API units, and the mass fractions of U are 2.71–25.50 ppm (average: 9.88 ppm) (**Figure 5**). In summary, the GR value and U content increase gradually from the bottom of the Wufeng Formation to its Guanyinqiao Member, peak in the Guanyinqiao Member, and then decrease gradually going further up to the Longmaxi Formation (**Figure 5**).

4.4 Spectral Analysis

The TOC content and GR values in shales are strongly positively correlated (**Figure 5**). Organic matter-rich shales generally have relatively high GR values. Therefore, GR data series obtained from dense sampling sites are used in this study to perform spectral analysis and examine the orbital control on organic matter enrichment.

GR well logs may contain interference signals unrelated to geological factors. To better identify orbital cycles from the GR well logs, we removed the effects of the deformation of the low-frequency portions of the well log data for the Wufeng Formation and the lower Longmaxi Formation using the "Detrending" module in the Acycle 2.3.1 software package before spectral analysis (**Figures 6A,B**).

We subjected the detrended GR well log data for the Wufeng and lower Longmaxi Formations to multitaper-method spectral analysis. Analysis of the multitaper-method spectrum for the Wufeng Formation reveals that the sedimentary cycle thickness corresponding to the peak power is 1.60 m (90% confidence interval, 1.03–2.29 m) (**Figure 7A**). Analysis of the multitaper-

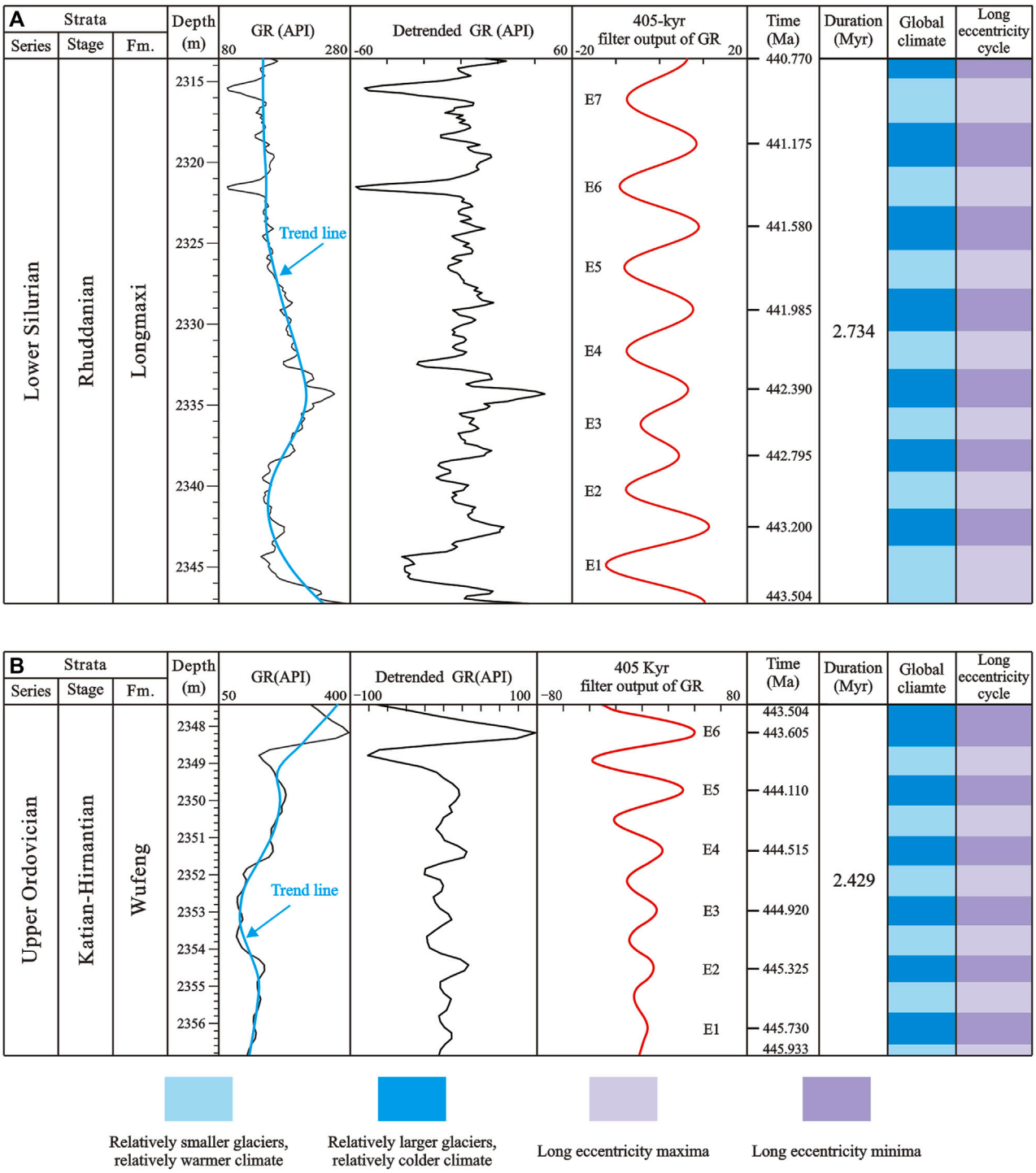

FIGURE 6 | Detrended GR data series and long eccentricity curves obtained through filtering of the detrended GR for the **(A)** lower Longmaxi Formation and **(B)** Wufeng Formation in well N211 in the Upper Yangtze Region. GR data series were detrended by subtracting 25% weighted averages. (E: 405-kyr long eccentricity).

method spectrum for the lower Longmaxi Formation reveals that the sedimentary cycle thicknesses corresponding to the peak powers are 5.64, 4.83, 3.26, 1.47, and 1.16 m, respectively, each with a confidence level of greater than 90% (**Figure 7B**).

To identify how the principal frequency varies with depth (i.e., the principal cycle) in the Wufeng and lower Longmaxi Formations and to ascertain the principal cycle stability with respect to depth, we subjected the GR curves for the Wufeng and

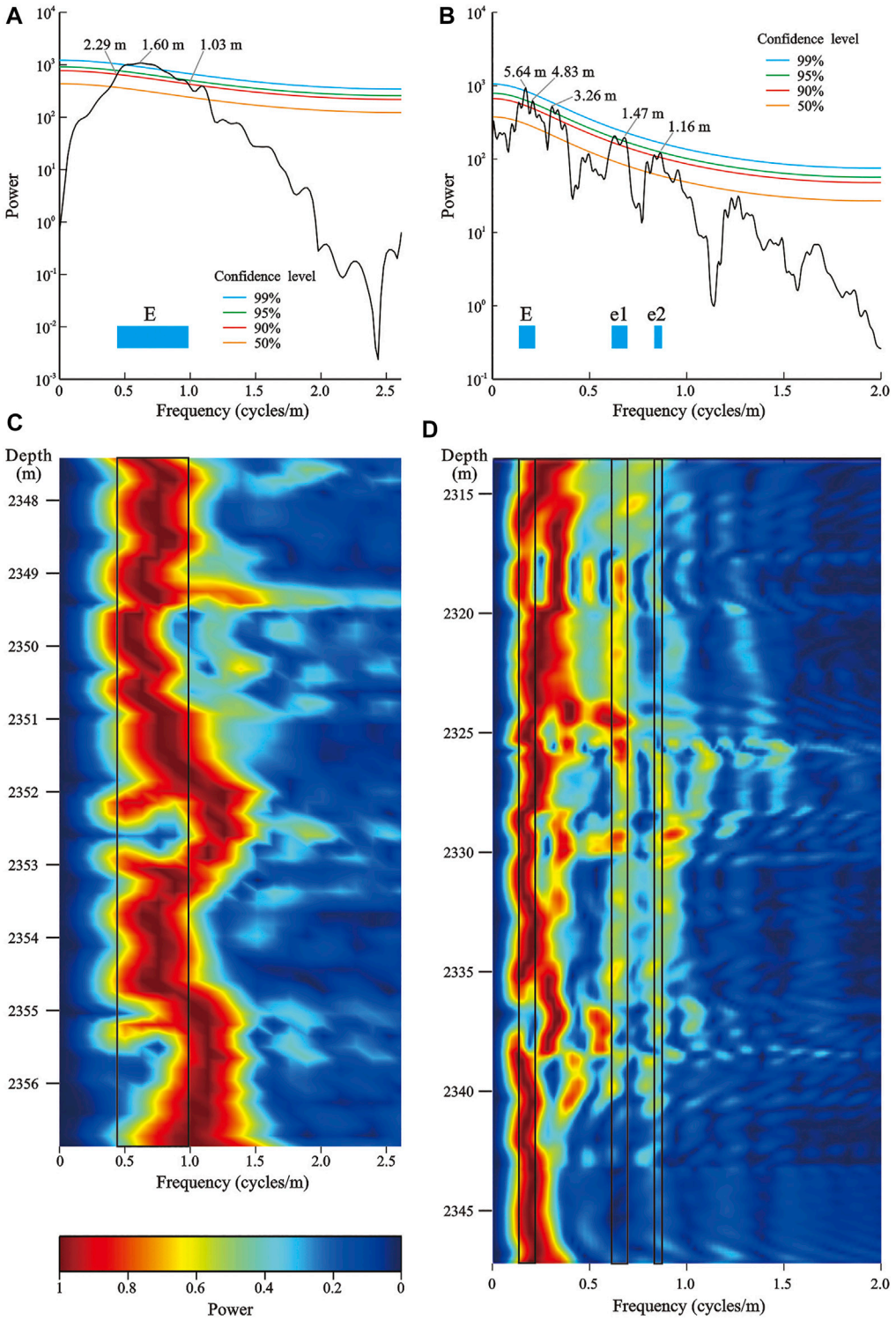

FIGURE 7 | Multitaper-method spectra and fast-Fourier transform sliding-window spectra produced from the GR data series for the Wufeng Formation (**A** and **C**, respectively) and the lower Longmaxi Formation (**B** and **D**, respectively) in well N211 of the Upper Yangtze Region.

lower Longmaxi Formations in well N211 to fast-Fourier transform sliding-window spectral analysis at a window step size of 0.1524 m and sliding-window lengths of 2 and 8 m, respectively. Analysis of the fast-Fourier transform sliding-window spectra reveals that the frequencies corresponding to high powers are consistent with those corresponding to the peak powers in the multitaper-method spectra

(**Figures 7C,D**), suggesting that principal frequency signals are preserved in each depth section of the Wufeng and lower Longmaxi Formations.

5 DISCUSSION

5.1 Cyclostratigraphy of the Wufeng–Longmaxi Formation Black Shales

A 405-kyr long eccentricity cycle is considered to have remained constant throughout geological time (Laskar et al., 2011; Ma et al., 2014; Ma et al., 2017). Jin S. et al. (2021) identified short eccentricity cycles of 125 and 95 kyr from the Upper Ordovician Wufeng Formation and the Lower Silurian Longmaxi Formation, respectively. Waltham (2015) accurately calculated Early Silurian (440 Ma) orbital parameters—obliquity: 33.4 ± 3.8 kyr; precession: 20.9 ± 1.5, 19.9 ± 1.3, 17.1 ± 1.0, and 17.2 ± 1.0 kyr. Hence, 405:125:95:33.4:20.4:17.15 is treated as the ratio of Earth's orbital parameter cycle in the Late Ordovician–Early Silurian. The ratio of the sedimentary cycle thickness corresponding to the peak power (at a high level of confidence) in spectral analysis is compared with this theoretical ratio of the orbital parameter cycle to ascertain the presence of orbital records in the GR data series for the Wufeng and lower Longmaxi Formations in well N211.

The sedimentary cycle thickness corresponding to a cycle of orbital parameters can be identified only if it is greater than four times the data point interval (Weedon, 2003; Wu et al., 2011). The deposition rate of the Wufeng Formation is calculated based on its isotopic age to be 2.56–3.04 m/Myr. Multiplying this deposition rate by the duration of each of the abovementioned orbital parameters yields the possible corresponding formation thickness. A comparison of the results with four times the data point interval (0.1542 m) reveals that only long eccentricity cycles can be identified from the GR data for the Wufeng Formation. Similarly, long eccentricity and short eccentricity cycles can be identified from the GR data of the lower Longmaxi Formation in well N211, whereas obliquity and precession cycles cannot.

Assuming that 1.03- to 2.29-m-thick sedimentary cycles in the Wufeng Formation correspond to the 405-kyr long eccentricity cycle, the deposition rate of the shales is estimated to be 2.6–5.7 m/Myr, which is similar to that (2.56–3.04 m/Myr) calculated from the isotopic age of the formation. We can conclude that the 1.03- to 2.29-m-thick sedimentary cycles correspond to the long eccentricity cycle during the deposition of the Wufeng Formation in well N211 (**Figures 7A,C**). The 4.83–5.64 m:1.47 m:1.16 m ratio (4.83–5.64:1.47:1.16 = 4.17–4.87:1.27:1) is very close to the long eccentricity:short eccentricity cycle ratio (405:125:95 = 4.27:1.32:1). Therefore, the 5.64–4.83-, 1.47-, and 1.16-m-thick sedimentary cycles may correspond to the long eccentricity cycle, 125-kyr short eccentricity cycle, and 95-kyr short eccentricity cycle in the lower Longmaxi Formation, respectively (**Figures 7B,D**). Based on the orbital cycles corresponding to these sedimentary cycles, the shale deposition rate is estimated at 11.76–14.00 m/Myr, which is similar to that (9.56–11.01 m/Myr) calculated from the isotopic age of the formation, which validates the above assumption.

Based on the spectral analysis, the sedimentary cycles (with a thickness of 4.83 m) corresponding to the 405-kyr long eccentricity cycle recorded in the lower Longmaxi Formation were extracted using a Gaussian bandpass filter with a frequency of 0.21 ± 0.04 cycles/m. The filtering results show that approximately seven long eccentricity cycles are recorded in the lower Longmaxi Formation in well N211 (**Figure 6A**). Similarly, the sedimentary cycles (with a thickness of 1.60 m) corresponding to the 405-kyr long eccentricity cycles recorded in the Wufeng Formation were extracted using a Gaussian bandpass filter with a frequency of 0.63 ± 0.12 cycles/m. The filtering results show that approximately six long eccentricity cycles are recorded in the Wufeng Formation in well N211 (**Figure 6B**). Following these filters, we can construct a floating astronomical time scale (ATS) using the interpreted 405-kyr long eccentricity cycles of the GR series. The age of the top Rhuddanian (440.77 ± 1.2 Ma) (Gradstein et al., 2012) can be used as a reference point. The floating ATS of the lower Longmaxi Formation ranges from 443.504 Ma to 440.770 Ma, and that of the Wufeng Formation ranges from 445.933 Ma to 443.504 Ma. Therefore, we can estimate a duration of approximately 5.163 Myr for the deposits of the Wufeng Formation and lower Longmaxi Formation (Upper Katian–Rhuddanian) (the durations of the Wufeng Formation and the lower Longmaxi Formation are approximately 2.429 Myr and 2.734 Myr, respectively) (**Figures 6A,B**). This value is in the range of the duration (447.62 ± 1.1 to 440.77 ± 1.2) estimates provided by Chen et al. (2015) and Gradstein et al. (2012). The result we obtained from this study provides an important refinement of the Late Katian–Rhuddanian stratigraphy.

5.2 Paleoenvironmental Modes During the Deposition of the Wufeng–Longmaxi Formation Black Shales

In the Late Ordovician through the Early Silurian, the Yangtze Block was located near the equator on the eastern margin of the Proto-Tethys Ocean, was situated within the southeasterly or northeasterly trade-wind zone on the west side of Gondwana, and was a semioccluded sea with a westward opening (i.e., the present-day northern margin of the Upper Yangtze Region was its western margin in the Late Ordovician through the Early Silurian) (**Figures 1A–C**) (Metcalfe, 1994; Li et al., 2005; Huang et al., 2018). The palaeogeographic location of the Yangtze Block is comparable to the location of the present-day coastal regions near the equator on the west side of the continent (i.e., the east side of the ocean). The oceanic and climatic conditions and paleoenvironmental mode during the deposition of the black shales in the Wufeng–Longmaxi Formation may have been similar to those in the present-day coastal regions near the equator on the west side of the continent. These coastal regions are located within the southeasterly or northeasterly trade-wind zone where offshore winds are formed. Offshore winds cause a loss of surface seawater by generating westward surface offshore currents in these coastal regions. Intermediate-

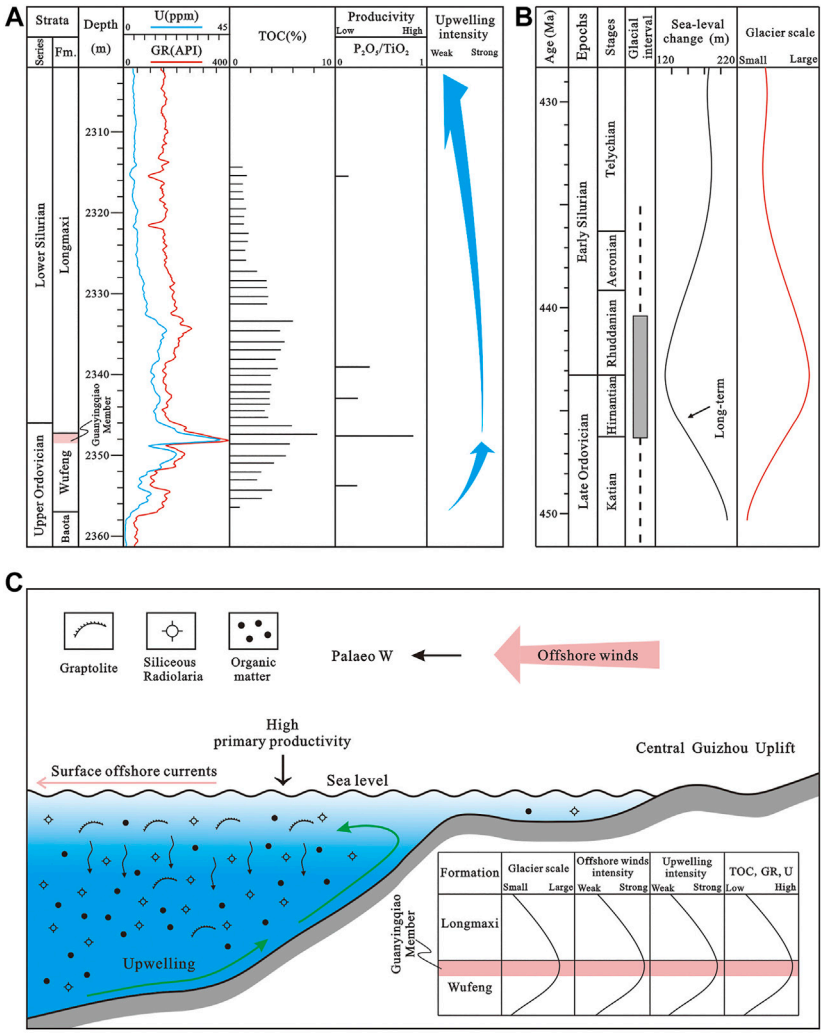

FIGURE 8 | (A) Vertical variations in the GR value, TOC content, and productivity metric (i.e., the P_2O_5/TiO_2 ratio) of the Wufeng–Longmaxi Formation black shales in well N211 and the upwelling intensity [data for the P_2O_5/TiO_2 ratio were obtained from Wang et al. (2017), and the upwelling intensity is from Zhao et al. (2019)]. **(B)** Glacier development and global sea-level change during the Late Ordovician–early Silurian, according to Haq and Schutter (2008). **(C)** Paleoenvironmental mode during the deposition of the Wufeng–Longmaxi Formation black shales in the Upper Yangtze Region.

depth and deep water in the ocean rise to compensate for the lost water in the coastal regions, forming upwelling currents (Schweigger, 1958; Huyer et al., 1987; Blanco et al., 2002; Capet et al., 2004; Chavez and Messié, 2009).

The Wufeng Formation and the lower Longmaxi Formation deposited in shallow water in the Upper Yangtze Region contain extensive records of storm deposits, including rip-up clasts deposited by proximal storms, hummocky cross-beds deposited by distal storms, and storm-scoured surfaces (Cheng and Wang, 1991; Li, 1997; Zhou et al., 2014), suggesting that storms were prevalent during the deposition of the black shales in the Wufeng–Longmaxi Formation in the Upper Yangtze Region. Multiple layers of potash bentonite are present in the black shales of the Wufeng–Longmaxi Formation in the Yangtze Block (**Figure 2C**). They are a product of the deposition and alteration of volcanic ash (Hu et al., 2009; Su et al., 2009; Yang X. et al., 2021; Du et al., 2021; Shen et al., 2021) generated by volcanic activity on the southeastern margin of the Yangtze Block (Su et al., 2009). The thickness of the potash bentonite in the black shales shows a gradual decrease from the southern margin to the northern margin of the Yangtze Block (Su et al., 2009). The main driver of the drift of the volcanic ash through the air is winds. Therefore, the origin of the volcanic ash and the distribution of the potash bentonite in the Yangtze Block suggest the presence of offshore winds travelling from the southern margin of the Yangtze Block to the northern margin during the deposition of the black shales in the Wufeng–Longmaxi Formation.

Siliceous organisms are an important indicator of upwelling zones (Leinen et al., 1986). The profusion of biogenic siliceous fossils in the black shales of the Wufeng–Longmaxi Formation suggests the presence of upwelling currents in the Upper Yangtze Region

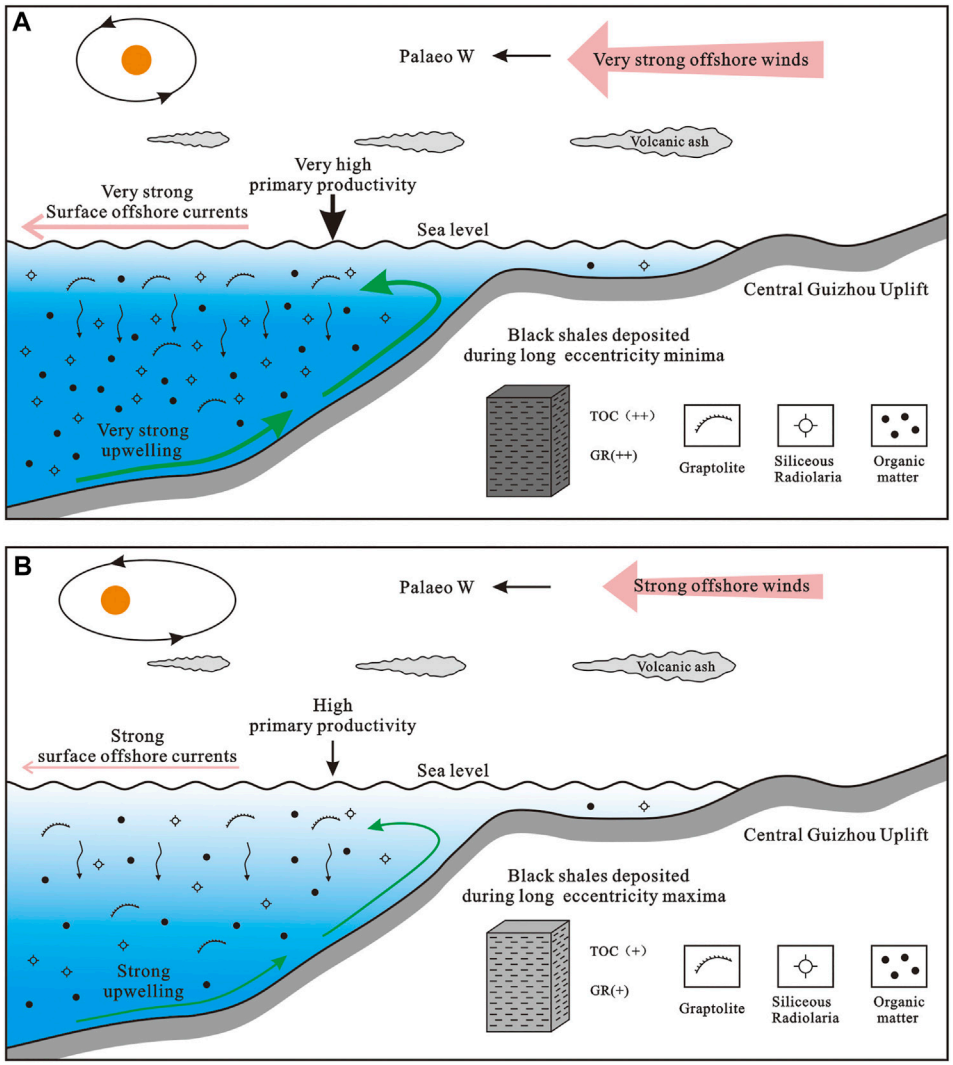

FIGURE 9 | Paleoenvironmental modes during the deposition of the Wufeng–Longmaxi Formation black shales at an orbital scale. **(A)** Paleoenvironmental mode during long eccentricity minima. **(B)** Paleoenvironmental mode during long eccentricity maxima.

(**Figures 4A,B**). Based on palaeontological, mineralogical, and geochemical evidence, previous researchers have noted that upwelling occurred during the deposition of the black shales of the Wufeng–Longmaxi Formation in the Upper Yangtze Region (Zhao et al., 2019; Yang S. et al., 2021; Zan et al., 2021). The upwelling currents brought nutrients to the upper Yangtze Sea and therefore considerably improved its sea-surface primary productivity. The flourishing, death, and decay of organisms consumed oxygen and thereby promoted the formation of an anoxic environment in the bottom seawater or the porewater in the sediments. High productivity and the anoxic environment together contributed to organic matter enrichment in the black shales of the Wufeng–Longmaxi Formation. The upwelling grew gradually more intensely from the early and middle stages of deposition of the Wufeng Formation to the depositional period of the Guanyinqiao Member and peaked during the deposition of the Guanyinqiao Member, followed by a gradual decrease during the deposition of the black shales in the Longmaxi Formation (**Figure 8A**) (Zhao et al., 2019; Yang S. et al., 2021). The vertical variation in the TOC content, GR value, U content, and productivity metric (i.e., the P_2O_5/TiO_2 ratio) reveals that these attributes increase gradually from the bottom of the Wufeng Formation to its top, peak at the Guanyinqiao Member, and decrease gradually going further up to the Longmaxi Formation (**Figures 5**, **8A**), which shows a similar pattern with upwelling intensity characterized by an initial increase followed by a decrease (**Figure 8A**).

Based on the above analysis, the paleoenvironmental modes during the deposition of the black shales in the Wufeng–Longmaxi Formation in the Upper Yangtze Region can be established. Under the influence of southeasterly or northeasterly trade winds, westward surface currents formed in the seawater in the Upper Yangtze Region, resulting in a loss of surface seawater. The intermediate-depth and deep water in the Proto-Tethys Ocean rose as compensation currents in the

upper Yangtze Sea via the western margin of the Upper Yangtze Region (i.e., its present-day northern margin), forming upwelling currents. This mechanism raised the surface primary productivity of the sea and promoted organic matter enrichment in the sediments (**Figure 8C**). During glacial periods, trade winds over the upwelling zone on the east side of the ocean intensified, thereby increasing the upwelling intensity (Abrantes, 1991; Weber et al., 1995; Wells and Okada, 1996; Kim et al., 2003; Romero et al., 2008; Matsuzaki et al., 2011). For example, the prevalent La Niña conditions and intensified southeasterly trade winds near the equator during the last glacial period resulted in stronger upwelling currents on the eastern margin of the ocean near the equator (Patrick and Thunell, 1997; Pisias and Mix, 1997; Mix et al., 1999; Feldberg and Mix, 2002; Kim et al., 2003; Martinez et al., 2003; Dubois et al., 2009), which might be related to the increase in the pole–equator temperature gradient or the intensification of the Walker circulation during the glacial period (Andreasen and Ravelo, 1997). The deposition of the black shales in the Wufeng–Longmaxi Formation corresponded to the glacial development-to-shrink process during the Late Ordovician to the early Silurian (**Figure 8B**) (Haq and Schutter, 2008). The Guanyinqiao Member in the Upper Yangtze Region was deposited in concurrence with the lowest sea level during the deposition of the black shales in the Wufeng–Longmaxi Formation, the most intensive Antarctic glacial development (Brenchley et al., 2003; Haq and Schutter, 2008; Rong et al., 2010). Therefore, during the deposition of the Guanyinqiao Member, the Upper Yangtze Region saw its strongest offshore winds and upwelling currents and peak marine productivity. The TOC content in the Guanyinqiao Member also shows a peak value (**Figure 8C**). Similarly, during the deposition of the Wufeng Formation from bottom to top, global glaciers gradually developed, and the TOC content of the Wufeng Formation therefore gradually increased from bottom to top (**Figures 8A–C**). During the deposition of the Longmaxi Formation from bottom to top, global glaciers gradually melted, and the TOC content of the Longmaxi Formation therefore gradually decreased from bottom to top (**Figures 8A–C**).

5.3 Orbital Control on Organic Matter Enrichment in the Wufeng–Longmaxi Formation Black Shales

In this study, the effects of a long eccentricity cycle on organic matter enrichment in black shales are analysed based on the long eccentricity cycles derived from the Wufeng Formation and the lower Longmaxi Formation in well N211.

The established paleoenvironmental mode of the Upper Yangtze Region provides a basis for discussing the effects of a long eccentricity cycle on organic matter enrichment. As mentioned in **Section 5.2**, the paleoenvironmental mode during the deposition of the black shales in the Wufeng–Longmaxi Formation in the Upper Yangtze Region was related to the glacial period. The development of upwelling in the Upper Yangtze Region promoted the enrichment of organic matter in shales. Strong upwelling occurred in the colder period of the Earth in the Upper Yangtze Region (**Figures 8A–C**). Therefore, the black shales of the Wufeng–Longmaxi Formation deposited when Earth was cold are richer in organic matter (**Figures 8A–C**).

During the deposition of the Wufeng–Longmaxi Formation black shales, periodic changes in long eccentricity led to periodic changes in the amount of solar radiation received by Earth, which in turn led to changes in cold and warm conditions (or changes in glacier size) in long eccentricity cycles (Zou et al., 2016; Cao et al., 2021). According to the paleoenvironmental model during the deposition of the Wufeng–Longmaxi Formation black shales in the Upper Yangtze Region, the changes in cold and warm conditions in long eccentricity cycles lead to periodic changes in the strength of upwelling in the Upper Yangtze Region and then affect the enrichment of organic matter in the Wufeng–Longmaxi Formation black shales. During long eccentricity minima, glaciers were formed at a relatively large scale (Zou et al., 2016; Cao et al., 2021); therefore, the offshore winds in the Upper Yangtze Region near the equator were relatively strong, resulting in the formation of relatively strong upwelling currents and a relatively high TOC content in the black shales, which is reflected by their relatively high GR values (**Figures 6**, **9A**). During long eccentricity maxima, glaciers were formed at a relatively small scale (Zou et al., 2016; Cao et al., 2021); therefore, the offshore winds and upwelling currents in the Upper Yangtze Region were relatively weak, resulting in relatively low TOC contents in the black shales, which is reflected by relatively low GR values (**Figures 6**, **9B**). Analysis of the controlling effects of the long eccentricity cycle on organic matter enrichment in the black shales of the Wufeng–Longmaxi Formation reveals a higher level of organic matter enrichment in the black shales deposited during long eccentricity minima. This understanding can provide a basis for predicting the distribution of shale with high organic matter abundance.

6 CONCLUSION

1) The black shales in the Wufeng Formation and the lower Longmaxi Formation in the Upper Yangtze Region are abundant in biogenic siliceous matter and framboidal pyrite.
2) TOC content, GR value, and U content increase gradually from the bottom of the Wufeng Formation to the Guanyinqiao Member, peak at the Guanyinqiao Member, and then decrease gradually going further up to the lower Longmaxi Formation.
3) Long eccentricity cycles can be identified from the GR curve for the Wufeng Formation in well N211 in the Upper Yangtze Region, and they correspond to sedimentary cycle thicknesses of 1.03–2.29 m. Approximately six long eccentricity cycles are recorded in the Wufeng Formation. Long eccentricity and short eccentricity cycles can be identified from the GR curve for the lower Longmaxi Formation. The long eccentricity cycle corresponds to sedimentary cycle thicknesses of 4.83–5.64 m, while the 125- and 95-kyr short eccentricity cycles correspond to sedimentary cycle thicknesses of 1.47 and 1.16 m, respectively. Approximately seven long eccentricity cycles are recorded in the lower Longmaxi Formation.

4) The black shales of the Wufeng–Longmaxi Formation in the Upper Yangtze Region deposited when Earth was relatively cold are richer in organic matter. At long eccentricity minima, the offshore winds in the Upper Yangtze Region were relatively strong, resulting in the formation of relatively strong upwelling currents, which led to a relatively high TOC content in the black shales. At long eccentricity maxima, the upwelling currents were weaker, resulting in lower TOC content in the black shales.

DATA AVAILABILITY STATEMENT

The original contributions presented in the study are included in the article/**Supplementary Material**. Further inquiries can be directed to the corresponding author.

AUTHOR CONTRIBUTIONS

SZ completed the writing and editing of the article. YL designed the research and focused on the scientific issues involved in the article. ZN provided the shale samples. YX, LC, and LZ performed the data analyses and prepared the figures and tables. All authors contributed to the article and approved the submitted version.

FUNDING

This work was supported by the Free Inquiry Fund of the State Key Laboratory of Oil and Gas Reservoir Geology and Exploitation (Chengdu University of Technology) (No. SKL2019015), the Science Foundation of the CNPC Chuanqing Drilling Company (No. CQCDLG-2020-02), and the Foundation of the State Key Laboratory of Petroleum Resources and Prospecting, China University of Petroleum, Beijing (No. PRP/open-2104).

SUPPLEMENTARY MATERIAL

The Supplementary Material for this article can be found online at: https://www.frontiersin.org/articles/10.3389/feart.2022.938323/full#supplementary-material

REFERENCES

Abrantes, F. (1991). Increased Upwelling off Portugal during the Last Glaciation: Diatom Evidence. *Mar. Micropaleontol.* 17 (3–4), 285–310. doi:10.1016/0377-8398(91)90017-z

Andreasen, D. J., and Ravelo, A. C. (1997). Tropical Pacific Ocean Thermocline Depth Reconstructions for the Last Glacial Maximum. *Paleoceanography* 12 (3), 395–413. doi:10.1029/97pa00822

Blanco, J. L., Carr, M. E., Thomas, A. C., and Strub, P. T. (2002). Hydrographic Conditions off Northern Chile during the 1996-1998 La Niña and El Niño Events. *J. Geophys. Res.* 107 (C3), 3017. doi:10.1029/2001jc001002

Bond, D. P. G., and Wignall, P. B. (2010). Pyrite Framboid Study of Marine Permian-Triassic Boundary Sections: a Complex Anoxic Event and its Relationship to Contemporaneous Mass Extinction. *Geol. Soc. Am. Bull.* 122 (7–8), 1265–1279. doi:10.1130/b30042.1

Brenchley, P. J., Carden, G. A., Hints, L., Kaljo, D., Marshall, J. D., Martma, T., et al. (2003). High-resolution Stable Isotope Stratigraphy of Upper Ordovician Sequences: Constraints on the Timing of Bioevents and Environmental Changes Associated with Mass Extinction and Glaciation. *Geol. Soc. Am. Bull.* 115 (1), 89–104. doi:10.1130/0016-7606(2003)115<0089:hrsiso>2.0.co;2

Cao, M. M., Wang, Z. X., Sui, Y., Li, Y. Z., Zhang, Z., Xiao, A. G., et al. (2021). Mineral Dust Coupled with Climate-Carbon Cycle on Orbital Timescales over the Past 4 Ma. *Geophys. Res. Lett.* 48 (18), 2021GL095327. doi:10.1029/2021gl095327

Capet, X. J., Marchesiello, P., and McWilliams, J. C. (2004). Upwelling Response to Coastal Wind Profiles. *Geophys. Res. Lett.* 31 (13), L13311. doi:10.1029/2004gl020123

Chavez, F. P., and Messié, M. (2009). A Comparison of Eastern Boundary Upwelling Ecosystems. *Prog. Oceanogr.* 83 (1–4), 80–96. doi:10.1016/j.pocean.2009.07.032

Chen, X., Bergström, S. M., Zhang, Y. D., and Wang, Z. H. (2013). A Regional Tectonic Event of Katian (Late Ordovician) Age across Three Major Blocks of China. *Chin. Sci. Bull.* 58 (34), 59–65. doi:10.1007/s11434-013-5990-0

Chen, X., Fan, J. X., Zhang, Y. D., Wang, H. Y., Chen, Q., Wang, W. H., et al. (2015). Subdivision and Delineation of the Wufeng and Lungmachi Black Shales in the Subsurface Areas of the Yangtze Platform. *J. Stratigr.* 39 (4), 351–358. (in Chinese with English abstrat). doi:10.19839/j.cnki.dcxzz.2015.04.001

Chen, X., Rong, J. Y., Li, Y., and Boucot, A. J. (2004). Facies Patterns and Geography of the Yangtze Region, South China, through the Ordovician and Silurian Transition. *Palaeogeogr. Palaeoclimatol. Palaeoecol.* 204 (3–4), 353–372. doi:10.1016/S0031-0182(03)00736-3

Cheng, H. J., and Wang, Y. Z. (1991). The Feature of Sedimentary Rocks Near the Ordovician-Silurian Boundary of the Fucheng Area, Nanzheng County, Shanxi Province. *J. Xi'an Coll. Geol.* 13 (3), 1–7. (in Chinese with English abstrat).

Cheng, L., Wang, J., Wan, Y., Fu, X., and Zhong, L. (2017). Astrochronology of the Middle Jurassic Buqu Formation (Tibet, China) and its Implications for the Bathonian Time Scale. *Palaeogeogr. Palaeoclimatol. Palaeoecol.* 487, 51–58. doi:10.1016/j.palaeo.2017.08.018

Cocks, L. R. M., and Torsvik, T. H. (2002). Earth Geography from 500 to 400 Million Years Ago: A Faunal and Palaeomagnetic Review. *J. Geol. Soc.* 159 (6), 631–644. doi:10.1144/0016-764901-118

Du, X., Jia, J., Zhao, K., Shi, J., Shu, Y., Liu, Z., et al. (2021). Was the Volcanism during the Ordovician-Silurian Transition in South China Actually Global in Extent? Evidence from the Distribution of Volcanic Ash Beds in Black Shales. *Mar. Petroleum Geol.* 123, 104721. doi:10.1016/j.marpetgeo.2020.104721

Dubois, N., Kienast, M., Normandeau, C., and Herbert, T. D. (2009). Eastern Equatorial Pacific Cold Tongue during the Last Glacial Maximum as Seen from Alkenone Paleothermometry. *Paleoceanography* 24 (4), PA4207. doi:10.1029/2009pa001781

Feldberg, M. J., and Mix, A. C. (2002). Sea-surface Temperature Estimates in the Southeast Pacific Based on Planktonic Foraminiferal Species: Modern Calibration and Last Glacial Maximum. *Mar. Micropaleontol.* 44 (1–2), 1–29. doi:10.1016/s0377-8398(01)00035-4

Gambacorta, G., Menichetti, E., Trincianti, E., and Torricelli, S. (2018). Orbital Control on Cyclical Primary Productivity and Benthic Anoxia: Astronomical Tuning of the Telychian Stage (Early Silurian). *Palaeogeogr. Palaeoclimatol. Palaeoecol.* 495, 152–162. doi:10.1016/j.palaeo.2018.01.003

Gradstein, F. M., Ogg, J. G., Schmitz, M., and Ogg, G. (2012). *The Geologic Time Scale 2012*. Amsterdam: Elsevier, 489–558.

Haq, B. U., and Schutter, S. R. (2008). A Chronology of Paleozoic Sea-Level Changes. *Science* 322 (5898), 64–68. doi:10.1126/science.1161648

Hu, Y. H., Sun, W. D., Ding, X., Wang, F. Y., Ling, M. X., and Liu, J. (2009). Volcanic Event at the Ordovician-Silurian Boundary: The Message from K-Bentonite of Yangtze Block. *Acta Pet. Sin.* 25 (12), 3298–3308. (in Chinese with English abstrat).

Huang, B., Yan, Y., Piper, J. D. A., Zhang, D., Yi, Z., Yu, S., et al. (2018). Paleomagnetic Constraints on the Paleogeography of the East Asian Blocks during Late Paleozoic and Early Mesozoic Times. *Earth-Science Rev.* 186, 8–36. doi:10.1016/j.earscirev.2018.02.004

Huang, C. J., Hesselbo, S. P., and Hinnov, L. (2010). Astrochronology of the Late Jurassic Kimmeridge Clay (Dorset, England) and Implications for Earth System Processes. *Earth Planet. Sci. Lett.* 289 (1–2), 242–255. doi:10.1016/j.epsl.2009.11.013

Huang, H., He, D., Li, D., Li, Y., Zhang, W., and Chen, J. (2020). Geochemical Characteristics of Organic-Rich Shale, Upper Yangtze Basin: Implications for the Late Ordovician-Early Silurian Orogeny in South China. *Palaeogeogr. Palaeoclimatol. Palaeoecol.* 554, 109822. doi:10.1016/j.palaeo.2020.109822

Huyer, A., Smith, R. L., and Paluszkiewicz, T. (1987). Coastal Upwelling off Peru during Normal and El Niño Times, 1981-1984. *J. Geophys. Res.* 92 (C13), 14297–14307. doi:10.1029/jc092ic13p14297

Jin, C., Liao, Z., and Tang, Y. (2020). Sea-level Changes Control Organic Matter Accumulation in the Longmaxi Shales of Southeastern Chongqing, China. *Mar. Petroleum Geol.* 119, 104478. doi:10.1016/j.marpetgeo.2020.104478

Jin, S., Deng, H., Zhu, X., Liu, Y., Liu, S., and Fu, M. (2020). Orbital Control on Cyclical Organic Matter Accumulation in Early Silurian Longmaxi Formation Shales. *Geosci. Front.* 11 (2), 533–545. doi:10.1016/j.gsf.2019.06.005

Kim, J. H., Schneider, R. R., Mulitza, S., and Müller, P. J. (2003). Reconstruction of SE Trade-Wind Intensity Based on Sea-Surface Temperature Gradients in the Southeast Atlantic over the Last 25 Kyr. *Geophys. Res. Lett.* 30 (22), 2144. doi:10.1029/2003gl017557

Kochhann, M. V. L., Savian, J. F., Tori, F., Catanzariti, R., Coccioni, R., Frontalini, F., et al. (2021). Orbital Tuning for the Middle Eocene to Early Oligocene Monte Cagnero Section (Central Italy): Paleoenvironmental and Paleoclimatic Implications. *Palaeogeogr. Palaeoclimatol. Palaeoecol.* 577, 110563. doi:10.1016/j.palaeo.2021.110563

Laskar, J., Fienga, A., Gastineau, M., and Manche, H. (2011). La2010: a New Orbital Solution for the Long-Term Motion of the Earth. *Astron. Astrophys.* 532 (A89), 1–15. doi:10.1051/0004-6361/201116836

Leinen, M., Cwienk, D., Heath, G. R., Biscaye, P. E., Kolla, V., Thiede, J., et al. (1986). Distribution of Biogenic Silica and Quartz in Recent Deep-Sea Sediments. *Geol* 14 (3), 199–203. doi:10.1130/0091-7613(1986)14<199:dobsaq>2.0.co;2

Li, M., Hinnov, L., and Kump, L. (2019). Acycle: Time-Series Analysis Software for Paleoclimate Research and Education. *Comput. Geosciences* 127, 12–22. doi:10.1016/j.cageo.2019.02.011

Li, W. H. (1997). Petrological Characteristics of Radiolarian Silicalite and its Geological Significance of Lower Silurian in the Hanzhong Region. *Acta Sedimentol. Sin.* 15 (3), 171–174. (in Chinese with English abstrat).

Li, Y., Matsumoto, R., and Kershaw, S. (2005). Sedimentary and Biotic Evidence of a Warm-Water Enclave in the Cooler Oceans of the Latest Ordovician Glacial Phase, Yangtze Platform, South China Block. *Isl. Arc* 14 (1), 623–635. doi:10.1111/j.1440-1738.2005.00472.x

Li, Y., Zhang, T., Ellis, G. S., and Shao, D. (2017). Depositional Environment and Organic Matter Accumulation of Upper Ordovician-Lower Silurian Marine Shale in the Upper Yangtze Platform, South China. *Palaeogeogr. Palaeoclimatol. Palaeoecol.* 466, 252–264. doi:10.1016/j.palaeo.2016.11.037

Liu, Z., Algeo, T. J., Guo, X., Fan, J., Du, X., and Lu, Y. (2017). Paleo-Environmental Cyclicity in the Early Silurian Yangtze Sea (South China): Tectonic or Glacio-Eustatic Control? *Palaeogeogr. Palaeoclimatol. Palaeoecol.* 466, 59–76. doi:10.1016/j.palaeo.2016.11.007

Lourens, L., Hilgen, F., Shacklefton, N. J., Laskar, J., and Wilson, D. (2004). "The Neogene Period," in *A Geologic Time Scale 2004*. Editors F. Gradstein, J. Ogg, and A. Smith (Cambridge: Cambridge University Press), 409–440.

Luo, C., Wang, L. S., Shi, X. W., Zhang, J., Wu, W., Zhao, S. X., et al. (2017). Biostratigraphy of theWufeng to Longmaxi Formation at Well Ning 211 of Changning Shale Gas Field. *J. Stratigr.* 41 (2), 142–152. (in Chinese with English abstrat). doi:10.19839/j.cnki.dcxzz.2017.02.003

Ma, C., Meyers, S. R., Sageman, B. B., Singer, B. S., and Jicha, B. R. (2014). Testing the Astronomical Time Scale for Oceanic Anoxic Event 2, and its Extension into Cenomanian Strata of the Western Interior Basin (U.S.A.). *Geol. Soc. Am. Bull.* 126 (7–8), 974–989. doi:10.1130/b30922.1

Ma, C., Meyers, S. R., and Sageman, B. B. (2017). Theory of Chaotic Orbital Variations Confirmed by Cretaceous Geological Evidence. *Nature* 542 (7642), 468–470. doi:10.1038/nature21402

Ma, Y., Cai, X., and Zhao, P. (2018). China's Shale Gas Exploration and Development: Understanding and Practice. *Petroleum Explor. Dev.* 45 (4), 589–603. doi:10.1016/s1876-3804(18)30065-x

Martinez, I., Keigwin, L., Barrows, T. T., Yokoyama, Y., and Southon, J. (2003). La Niña-like Conditions in the Eastern Equatorial Pacific and a Stronger Choco Jet in the Northern Andes during the Last Glaciation. *Paleoceanography* 18 (2), 1033. doi:10.1029/2002pa000877

Matsuzaki, K. M. R., Eynaud, F., Malaizé, B., Grousset, F. E., Tisserand, A., Rossignol, L., et al. (2011). Paleoceanography of the Mauritanian Margin during the Last Two Climatic Cycles: from Planktonic Foraminifera to African Climate Dynamics. *Mar. Micropaleontol.* 79 (3–4), 67–79. doi:10.1016/j.marmicro.2011.01.004

Metcalfe, I. (1994). "Late Palaeozoic and Mesozoic Palaeogeography of Eastern Pangaea and Tethys," in *Pangea: Global Environments and Resources*. Editors A. F. Embry, B. Beauchamp, and D. J. Glass (Canada: Canadian Society of Petroleum Geologists), 97–111.

Mix, A. C., Morey, A. E., Pisias, N. G., and Hostetler, S. W. (1999). Foraminiferal Faunal Estimates of Paleotemperature: Circumventing the No-Analog Problem Yields Cool Ice Age Tropics. *Paleoceanography* 14 (3), 350–359. doi:10.1029/1999pa900012

Patrick, A., and Thunell, R. C. (1997). Tropical Pacific Sea Surface Temperatures and Upper Water Column Thermal Structure during the Last Glacial Maximum. *Paleoceanography* 12 (5), 649–657. doi:10.1029/97pa01553

Pisias, N. G., and Mix, A. C. (1997). Spatial and Temporal Oceanographic Variability of the Eastern Equatorial Pacific during the Late Pleistocene: Evidence from Radiolaria Microfossils. *Paleoceanography* 12 (3), 381–393. doi:10.1029/97pa00583

Rachold, V., and Brumsack, H. J. (2001). Inorganic Geochemistry of Albian Sediments from the Lower Saxony Basin NW Germany: Palaeoenvironmental Constraints and Orbital Cycles. *Palaeogeogr. Palaeoclimatol. Palaeoecol.* 174 (1), 121–143. doi:10.1016/s0031-0182(01)00290-5

Ravier, E., Martinez, M., Pellenard, P., Zanella, A., and Tupinier, L. (2020). The Milankovitch Fingerprint on the Distribution and Thickness of Bedding-Parallel Veins (Beef) in Source Rocks. *Mar. Petroleum Geol.* 122, 104643. doi:10.1016/j.marpetgeo.2020.104643

Romero, O. E., Kim, J. H., and Donner, B. (2008). Submillennial-to-millennial Variability of Diatom Production off Mauritania, NW Africa, during the Last Glacial Cycle. *Paleoceanography* 23 (3), PA3218. doi:10.1029/2008pa001601

Rong, J. Y., Chen, X., Zhan, R. B., Fan, J. X., Wang, Y., Zhang, Y. D., et al. (2010). New Observation on Ordovician-Siliurian Boundary Strata of Southern Tongzi County. Northern Guizhou, Southwest China. *J. Stratigr.* 34 (4), 337–348. (in Chinese with English abstrat). doi:10.19839/j.cnki.dcxzz.2010.04.001

Sageman, B. B., Meyers, S. R., and Arthur, M. A. (2006). Orbital Time Scale and New C-Isotope Record for Cenomanian-Turonian Boundary Stratotype. *Geol* 34 (2), 125–128. doi:10.1130/g22074.1

Schwarzacher, W. (1993). *Cyclostratigraphy and the Milankovitch Theory*. Amsterdam: Elsevier.

Schwarzacher, W. (1989). Milankovitch Cycles and the Measurement of Time. *Terra nova.* 1 (5), 405–408. doi:10.1111/j.1365-3121.1989.tb00400.x

Schweigger, E. (1958). Upwelling along the Coast of Peru. *J. Oceanogr. Soc. Jpn.* 14 (3), 87–91. doi:10.5928/kaiyou1942.14.87

Shen, J., Wang, P., Chen, K., Zhang, D., Wang, Y., Cai, Q., et al. (2021). Relationship between Volcanic Activity and Enrichment of Shale Organic Matter during the Ordovician-Silurian Transition in Western Hubei, Southern China. *Palaeogeogr. Palaeoclimatol. Palaeoecol.* 577, 110551. doi:10.1016/j.palaeo.2021.110551

Shi, J., Jin, Z., Liu, Q., and Huang, Z. (2020). Depositional Process and Astronomical Forcing Model of Lacustrine Fine-Grained Sedimentary Rocks: A Case Study of the Early Paleogene in the Dongying Sag, Bohai Bay Basin. *Mar. Petroleum Geol.* 113, 103995. doi:10.1016/j.marpetgeo.2019.08.023

Shi, J. Y., Jin, Z. J., Liu, Q. Y., Fan, T. L., and Gao, Z. Q. (2021). Sunspot Cycles Recorded in Eocene Lacustrine Fine-Grained Sedimentary Rocks in the Bohai Bay Basin, Eastern China. Global Planet. *Change* 205, 103614. doi:10.1016/j.gloplacha.2021.103614

Strasser, A., Hilgen, F. J., and Heckel, P. H. (2006). Cyclostratigraphy Concepts, Definitions, and Applications. *Newsl. Stratigr.* 42 (2), 75–114. doi:10.1127/0078-0421/2006/0042-0075

Su, W., Huff, W. D., Ettensohn, F. R., Liu, X., Zhang, J. E., and Li, Z. (2009). K-bentonite, Black-Shale and Flysch Successions at the Ordovician-Silurian Transition, South China: Possible Sedimentary Responses to the Accretion of

Cathaysia to the Yangtze Block and its Implications for the Evolution of Gondwana. *Gondwana Res.* 15 (1), 111–130. doi:10.1016/j.gr.2008.06.004

Tang, L., Song, Y., Jiang, S., Jiang, Z., Li, Z., Yang, Y., et al. (2020). Organic Matter Accumulation of the Wufeng-Longmaxi Shales in Southern Sichuan Basin: Evidence and Insight from Volcanism. *Mar. Petroleum Geol.* 120, 104564. doi:10.1016/j.marpetgeo.2020.104564

Waltham, D. (2015). Milankovitch Period Uncertainties and Their Impact on Cyclostratigraphy. *J. Sediment. Res.* 85 (8), 990–998. doi:10.2110/jsr.2015.66

Wang, H. Z. (1985). *Atlas of the Palaeogeography of China*. Beijing: Cartographic Publishing House. (in Chinese with English summary).

Wang, Y., Dong, D., Huang, J., Li, X., and Wang, S. (2016). Guanyinqiao Member Lithofacies of the Upper Ordovician Wufeng Formation Around the Sichuan Basin and the Significance to Shale Gas Plays, SW China. *Petroleum Explor. Dev.* 43 (1), 45–53. doi:10.1016/s1876-3804(16)30005-2

Wang, Y., Li, X., Dong, D., Zhang, C., and Wang, S. (2017). Major Controlling Factors for the High-Quality Shale of Wufeng-Longmaxi Formation, Sichuan Basin. *Energy Explor. Exploitation* 35 (4), 444–462. doi:10.1177/0144598717698080

Weber, M. E., Wiedicke, M., Riech, V., and Erlenkeuser, H. (1995). Carbonate Preservation History in the Peru Basin: Paleoceanographic Implications. *Paleoceanography* 10 (4), 775–800. doi:10.1029/95pa01566

Weedon, G. P., Coe, A. L., and Gallois, R. W. (2004). Cyclostratigraphy, Orbital Tuning and Inferred Productivity for the Type Kimmeridge Clay (Late Jurassic), Southern England. *J. Geol. Soc.* 161 (4), 655–666. doi:10.1144/0016-764903-073

Weedon, G. (2003). *Time-Series Analysis and Cyclostratigraphy*. Cambridge: Cambridge University Press.

Wells, P., and Okada, H. (1996). Holocene and Pleistocene Glacial Palaeoceanography off Southeastern Australia, Based on Foraminifers and Nannofossils in Vema Cored Hole V18-222*. *Aust. J. Earth Sci.* 43 (5), 509–523. doi:10.1080/08120099608728273

Wu, H. C., Zhang, S. H., Feng, Q. L., Fang, N. Q., Yang, T. S., and Li, H. Y. (2011). Theoretical Basis , Research Advancement and Prospects of Cyclostratigraphy. *Earth Sci. J. China Univ. Geosci.* 36 (3), 409–428. (in Chinese with English abstrat). doi:10.3799/j.cnki.dqkx.2011.045

Yan, D., Chen, D., Wang, Q., and Wang, J. (2009). Geochemical Changes across the Ordovician-Silurian Transition on the Yangtze Platform, South China. *Sci. China Ser. D-Earth Sci.* 52 (1), 38–54. doi:10.1007/s11430-008-0143-z

Yang, S., Hu, W., and Wang, X. (2021). Mechanism and Implications of Upwelling from the Late Ordovician to Early Silurian in the Yangtze Region, South China. *Chem. Geol.* 565, 120074. doi:10.1016/j.chemgeo.2021.120074

Yang, X., Yan, D., Zhang, B., Zhang, L., Wei, X., Li, T., et al. (2021). The Impact of Volcanic Activity on the Deposition of Organic-Rich Shales: Evidence from Carbon Isotope and Geochemical Compositions. *Mar. Petroleum Geol.* 128, 105010. doi:10.1016/j.marpetgeo.2021.105010

Yao, X., Zhou, Y., and Hinnov, L. A. (2015). Astronomical Forcing of a Middle Permian Chert Sequence in Chaohu, South China. *Earth Planet. Sci. Lett.* 422, 206–221. doi:10.1016/j.epsl.2015.04.017

Zan, B., Mou, C., Lash, G. G., Ge, X., Wang, X., Wang, Q., et al. (2021). An Integrated Study of the Petrographic and Geochemical Characteristics of Organic-Rich Deposits of the Wufeng and Longmaxi Formations, Western Hubei Province, South China: Insights into the Co-evolution of Paleoenvironment and Organic Matter Accumulation. *Mar. Petroleum Geol.* 132, 105193. doi:10.1016/j.marpetgeo.2021.105193

Zhang, X., Zhang, T., Zhao, X., Zhu, H., Mihai, E. P., Chen, L., et al. (2021). Effects of Astronomical Orbital Cycle and Volcanic Activity on Organic Carbon Accumulation during Late Ordovician-Early Silurian in the Upper Yangtze Area, South China. *Petroleum Explor. Dev.* 48 (4), 850–863. doi:10.1016/s1876-3804(21)60071-x

Zhao, S.-Z., Li, Y., Min, H.-J., Wang, T., Nie, Z., Zhao, Z.-Z., et al. (2019). Development of Upwelling during the Sedimentary Period of the Organic-Rich Shales in the Wufeng and Longmaxi Formations of the Upper Yangtze Region and its Impact on Organic Matter Enrichment. *J. Mar. Sci. Eng.* 7 (4), 99. doi:10.3390/jmse7040099

Zhong, Y., Wu, H., Fan, J., Fang, Q., Shi, M., Zhang, S., et al. (2020). Late Ordovician Obliquity-Forced Glacio-Eustasy Recorded in the Yangtze Block, South China. *Palaeogeogr. Palaeoclimatol. Palaeoecol.* 540, 109520. doi:10.1016/j.palaeo.2019.109520

Zhou, K. K., Mu, C. L., Liang, W., and Ge, X. Y. (2014). Tide-dominated Deltaic Deposits in Lungamachi Formation, Longshan-Yongshun Regions, Northwestern Hunan: The Initial Sedimentary Responses to Outset of "Xuefeng Uplift". *Acta Sedimentol. Sin.* 32 (3), 468–477. (in Chinese with English abstrat). doi:10.14027/j.cnki.cjxb.2014.03.010

Zhou, L., Algeo, T. J., Shen, J., Hu, Z., Gong, H., Xie, S., et al. (2015). Changes in Marine Productivity and Redox Conditions during the Late Ordovician Hirnantian Glaciation. *Palaeogeogr. Palaeoclimatol. Palaeoecol.* 420, 223–234. doi:10.1016/j.palaeo.2014.12.012

Zou, C. N., Zhu, R. K., Chen, Z. Q., Ogg, J. G., Wu, S. T., Dong, D. Z., et al. (2018). Organic-matter-rich Shales of China. *Earth-Science Rev.* 189, 51–78. doi:10.1016/j.earscirev.2018.12.002

Zou, Z., Huang, C., Li, M., and Zhang, Y. (2016). Climate Change Response to Astronomical Forcing during the Oligocene-Miocene Transition in the Equatorial Atlantic (ODP Site 926). *Sci. China Earth Sci.* 59, 1665–1673. doi:10.1007/s11430-016-5311-y

Conflict of Interest: Author ZN was employed by PetroChina Southwest Oil and Gas Field Company.

The remaining authors declare that the research was conducted in the absence of any commercial or financial relationships that could be construed as a potential conflict of interest.